Arch. Metall. Mater. **66** (2021), 1, 217-222

DOI: 10.24425/amm.2021.134778

TAO WANG[1], XUE GONG[2], SHUDE JI[2*], GANG XUE[1**], ZAN LV[2]

ULTRASONIC ASSISTED ACTIVE-PASSIVE FILLING FRICTION STIR REPAIRING TO ELIMINATE VOLUME DEFECTS

Ultrasonic assisted active-passive filling friction stir repairing (A-PFFSR) was proposed to repair volume defects in the metallic parts. Sound joints without interfacial defects could be achieved. Firstly, the ultrasonic was beneficial to improving material flow and atom diffusion, and then eliminated kissing bond defects compared to conventional A-PFFSR joints. Secondly, the equiaxed grains were refined by ultrasonic vibration. Lastly, the repairing passes were reduced due to the ultrasonic, which decreased softening degree of the repaired joints. The maximum tensile strength of 150 MPa was achieved. Therefore, this strategy to repair the volume defects is feasibility and potential in the remanufacturing fields of aerospace and transportation.

Keywords: Friction stir repairing, Magnesium alloys, Defects, Ultrasonic, Mechanical properties

1. Introduction

Up to present, metallic materials have been extensively used in the manufacturing fields such as aerospace, high-speed railway and shipping transportation, which attract extensive attentions in welding techniques [1-3]. After long service, corrosion, wear and the other severe environments are prone to cause crack, pitting, scratch defects and so on, which are detrimental to the service life of structural parts. Moreover, under inappropriate process parameters or technological conditions, welding defects easily form and deteriorate mechanical properties of the welded workpieces. Currently, all service lifetime of these structural parts is the "Manufacturing–Servicing–Scrap" process, and results in economic loss and material waste, which are detrimental to the development of circular economy. However, introducing repairing processes into service lifetime of structural parts can realize recycle service lifetime, as "Manufacturing–Servicing–Scrap–Repairing", which can significantly improve material utilization, resource conservation, energy-saving and emission-reduction. Green remanufacturing, with the advantages of high efficiency, low cost and little pollution, is a green repairing technology, which can restore and upgrade the properties of products via advanced manufacturing techniques. Friction stir welding (FSW) has the advantages of higher joint quality, smaller distortion and lower residual stress compared with conventional fusion welding [4-10]. Some researchers have reported the repairing processes via FSW.

According to the characteristics of the welding or exogenous source induced defects, the repairing processes are mainly composed of defect detecting, locating, regularizing and repairing. The global defects mainly contain surface peel, groove, tunnel, kissing bond and lack of root penetration defects, as well as surface damage and long crack induced by the exogenous source. The above-mentioned defects always form along a certain direction, which are primarily repaired by friction stir processing [11], vertical compensation FSW [12,13], re-FSW [14]. For the local defects such as keyhole, cavity and pitting, the digging and regularizing are essential due to the irregularly distributed inside the parts, in which the loss of the materials can be remedied by the additional filling materials. Friction plug welding (FPW) [15], friction bit joining (FBJ) [16], filling friction stir welding (FFSW) [17-19], active-passive filling friction stir repairing (A-PFFSR) [20,21], drilling-filling friction stir repairing (D-FFSR) [22] and passive filling friction stir repairing (PFFSR) [23] were proposed to eliminate the local volume defects and then achieve the satisfactory results. However, when improper welding parameters are selected, kissing bond and cavity defects are easily formed at the interfaces between base material (BM) and extra filling materials, which can be attributed to insufficient material flow and weak atom diffusion bonding generated by

[1] LUOYANG SHIP MATERIAL RESEARCH INSTITUTE, LUOYANG 471023, P. R. CHINA
[2] SHENYANG AEROSPACE UNIVERSITY, COLLEGE OF AEROSPACE ENGINEERING, SHENYANG 110136, P. R. CHINA
Corresponding authors: * superjsd@163.com, ** xuegang@725.com.cn

low peak temperature and pressure. Accordingly, the repairing process windows are narrowed to a small range.

Therefore, the repairing interfaces need be further improved by auxiliary processes. Nowadays, ultrasonic auxiliary FSW (UAFSW) is a popular process, which attracts extensive attentions [24-29]. Ma et al. [28] pointed that the addition of the ultrasonic could improve atom diffusion at the FSWed Al/Ti joining interface. Niu et al. [30] reported that the ultrasonic could improve the kinetic energy levels and diffusivity of atoms and enhance the plastic rheological behavior of the materials in the UAFSW joint of Al/Mg alloys. Liu et al. [31] found that the ultrasonic vibration could enhance material flow. Therefore, the ultrasonic during the repairing processes can improve the quality of repairing interfaces.

A-PFFSR, a solid state repairing process proposed by our research team, has successfully realized the high-quality repairing of Al or Mg alloys. However, the deeper the volume defects, the more the repairing passes. This easily results in possibility of defects occurrence and severe joint softening. Therefore, ultrasonic assisted A-PFFSR was proposed to repair the volume defects from the viewpoints of few repairing passes, free defects and high-quality repairing. Meanwhile, joint formation, microstructure evolution and mechanical properties of the repaired joints with and without the ultrasonic were compared.

2. Experimental procedures

4 mm thick AZ31B Mg alloy sheets were selected as the BM, whose dimension were 200 mm × 200 mm. Two pinless tools made of H13 tool steel were employed, which had the shoulder diameters of 10 mm and 14 mm, respectively. A tilting angle with relative to the Z-axis was 0. A rotating velocity of 1400 rpm was used referenced to the previous work. The type of FSW machine was FSW-3LM-4012, as shown in Fig. 1. An ultrasonic power and a constant frequency of the ultrasonic generator (TJS-3000) were 1600 W and 20 kHz. In this study, the ultrasonic was applied from the back side. The ultrasonic generator was 20 mm distance away from the repairing defect. The location of the ultrasonic has been optimized in the previous experiment, which can exert the biggest vibration effects. Moreover, the ultrasonic was applied in the whole process. Illustration of ultrasonic assisted A-PFFSR is displayed in Fig. 2. The A-PFFSR process can be divided into two stages: active filling and passive filling. During the active filling stage (Figs. 2a and b), a pinless tool with a 10 mm shoulder diameter was plunged, and materials surrounding the volume defects were driven into the bottom of the volume defect, forming active filling zone (AFZ). During the passive filling stage (Figs. 2c and d), an extra filling material into the volume defect was heated and stirred by the pinless tool with a 14 mm shoulder diameter. The volume defect was completely repaired and passive filling zone (PAZ) was formed. The A-PFFSR was performed by one time active filling and one time passive filling. Repairing passes were reduced from two times to one time active filling compared with the published papers [20,21]. During the A-PFFSR process, once the pinless tools contacted with the repairing materials, the ultrasonic was exerted to improve material flow around the repairing interfaces until to the retraction of the pinless tool. The six-spiral-flute shoulder was used, which has been verified to improve vertical flow of the material [20].

Microstructural and mechanical specimens were obtained vertical to the welding line by an electrical discharge cutting machine. The microstructural specimens were etched by an reagent

Fig. 1. FSW equipment with ultrasonic device

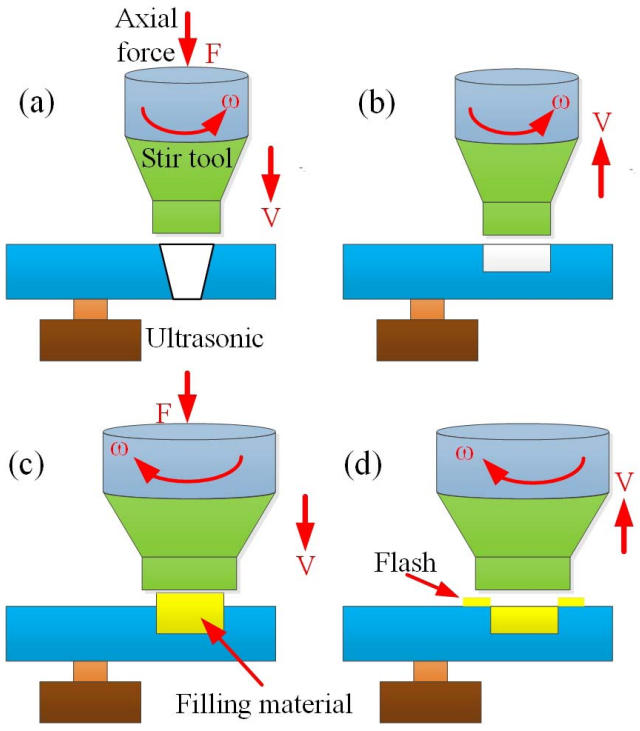

Fig. 2. Schematics of ultrasonic assisted A-PFFSR: (a) active filling, (b) active filling in the retracting stage, (c) passive filling in the pushing stage and (d) completion of ultrasonic assisted A-PFFSR

for the AZ31B alloy (25 ml CH_3COOH + 5 g $C_6H_2OH(NO_2)_3$ + 10 ml H_2O + 100 ml C_2H_5OH), and observed by an light microscope (Olympus-GX71). Microhardness of the repaired joint was measured by a microhardness tester (HVS-1000A) at a load of 200 g for 10 s along the thickness direction. Three tested layers along the thickness direction were measured. The interval between two adjacent points was defined as 0.5 mm (Fig. 3). Three tensile specimens were prepared for each joint according to GB/T 2651-2008 to evaluate tensile properties of the repaired joints (Fig. 4). The average value was presented for discussion. The tensile test was performed at room temperature at a constant crosshead speed of 2 mm/min (RG4300). Fracture surface of the tensile specimen was observed using a scanning electron microscope (Hitachi SU3500).

3. Results and discussion

Fig. 5 shows the macrostructures of the repaired joints. The repairing joint is composed of filling zone (FZ), thermo-mechanically affected zone (TMAZ), heat affected zone (HAZ) and BM. The FZ is further divided into AFZ and PFZ. It is observed from Figs. 5a and b that no interfacial defects form in the AFZ. This verifies that the materials below the pinless tool can be sufficiently plasticized during the active filling process and then form good metallurgical bonding with the rotating, plunging and forging of the pinless tool.

However, with the addition of the extra filling material during the passive filling stage, insufficient material flow is attained due to relatively larger thickness of the passive filling layer, which results in interfacial defects along the interfaces between the PFZ and the repairing parts (Fig. 6). The pinless tool can join the thin plates of Al alloys lower than 2 mm due to good plastic and flow abilities [32,33]. Huang et al. [34] only reported that the keyhole with a thickness of 1.5 mm could be repaired by the pinless tool. The successful repairing of the thicker Mg alloys plates higher than 1.5 mm has not been reported because of worse plastic deformability induced by the hexagonal close packed (HCP) crystal lattice. In Fig. 5b, the passive filling layer is higher than 1.5 mm, which is difficult to be repaired successfully. With the addition of the ultrasonic, the interfacial defects between the PFZ and the repairing parts are completely eliminated, as shown in Figs. 5a and b. This is because that the ultrasonic can significantly enhance material flow and atom

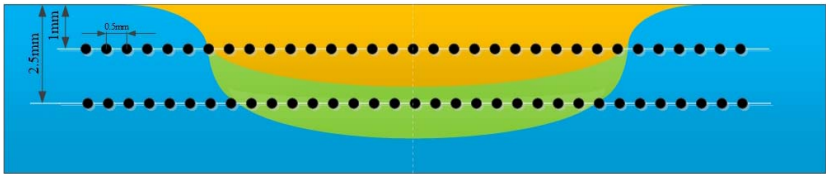

Fig. 3. Schematic of measurement points of the microhardness test

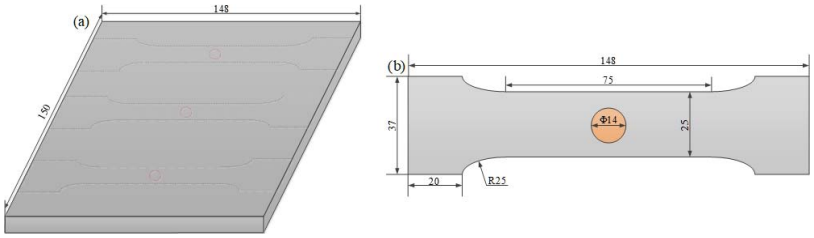

Fig. 4. Schematics: (a) test plate and (b) dimensions of tensile sample (unit: mm

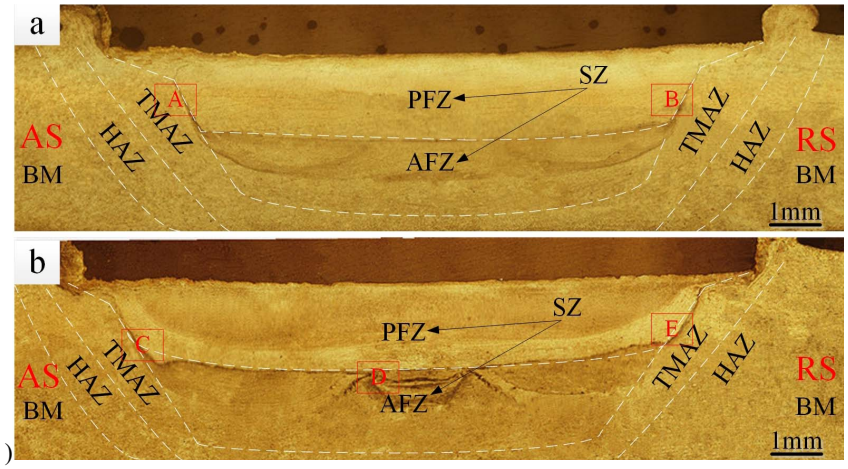

Fig. 5. Macrostructures of the repaired joints using two welding processes: (a) ultrasonic assisted A-PFFSR and (b) conventional A-PFFSR

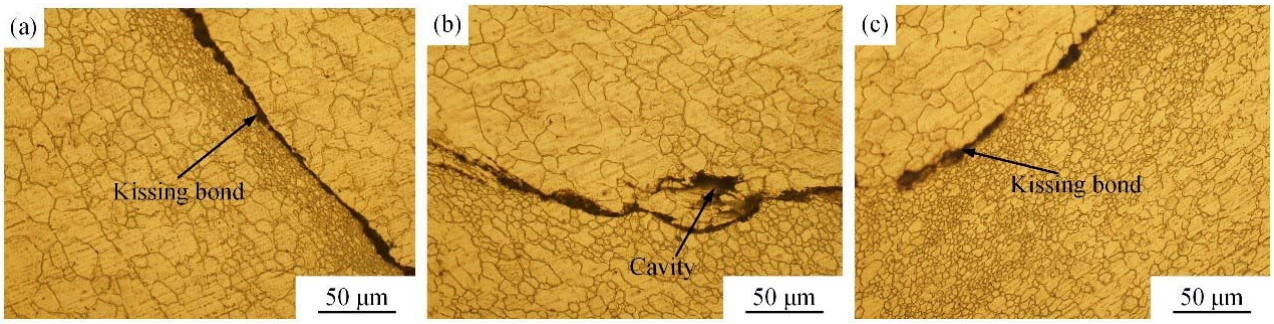

Fig. 6. Interfacial defects between PFZ and repairing parts: (a) C, (b) D and (c) E in Fig. 5b

diffusion. The elimination of the interfacial defects is beneficial to increasing the metallurgical bonding area and avoiding the crack initiation during tensile test. Moreover, the small weld-thinning of the repaired joint can be gained. Huang et al. [35] also stated that the non-weld-thinning FSW joint can improve mechanical properties.

Fig. 7 shows the microstructural morphologies of typical regions marked in Fig. 5a. During the active filling stage, the materials near the keyhole are stirred and then squeezed into the keyhole by the pinless tool. Because the ultrasonic can promote the grain refinement, a large grain refinement region occurs near the joining interfaces (Figs. 7a and b) under ultrasonic effects compared with the conventional process (Figs. 6a and b). During the passive filling stage, the pinless tool drives the extra passive filling materials flow via friction heat and stirring action, making the materials contact with the repairing interfaces. After the passive filling process, continuous metallurgical bonding occurs at the joining interfaces because the ultrasonic improves the atom diffusion. For the A-PFFSR process, the interfacial microstructures in Figs. 7a and b are more important than the others for improving mechanical properties, since the weak region always locates at the interfaces between the filling zones or between the filling zone and the BM. Therefore, the ultrasonic can improve the mechanical properties by eliminating the interfacial defects. The repairing passes have also been reduced, which can be beneficial to reducing the thermal cycle and then decrease the joint softening.

Fig. 8 shows the microhardness distribution of the typical joint using the ultrasonic assisted A-PFFSR. The microhardness distribution of the repaired joint presents a “W” shape, which is related to the grain size. The values in the AFZ are all higher than those in the PFZ due to finer grain sizes. The partial fluctuations presented in the AFZ and PFZ are mainly correlated with interfacial microstructures. In this study, the width of joining interfaces is very small, which is difficult to be measured. The hardness minima occurred in the HAZ but not the joining interface. Meanwhile, the microstructures in the weld center remained partial microstructures of the base material, resulting in relatively higher hardness values. Additionally, after passive filling process, the welding tool continued to move for a certain distance to guarantee the joint formation. The left side in Fig. 8 corresponded to the advancing side of the repairing joints, where the materials experienced high shear stress and peak temperature, and consequently resulting in the low hardness value.

Fig. 9 exhibits tensile results of the repaired joints using the two processes. With the addition of the ultrasonic, the tensile properties of the repaired joints are improved compared with those of conventional A-PFFSR joints. The maximum tensile strength and elongation of the repaired joints using ultrasonic assisted A-PFFSR are 150 MPa and 12.2%, which are all higher than those of conventional A-PFFSR joints. As a matter of fact, mechanical properties of the repaired joints are closely related to the interfacial microstructures and defects. During conventional A-PFFSR, insufficient material flow in the passive filling appears at the interfaces between the filling materials and the repaired parts, which easily results in the kissing bond or cavity defects. During tensile test, the interfacial defects are prone to reduce the area of load bearing and become the crack source. With the increase of the tensile load, these defects are further propagated along the crack until to the fracture. Because the ultrasonic effectively improves material flow behavior and diffusivity of the

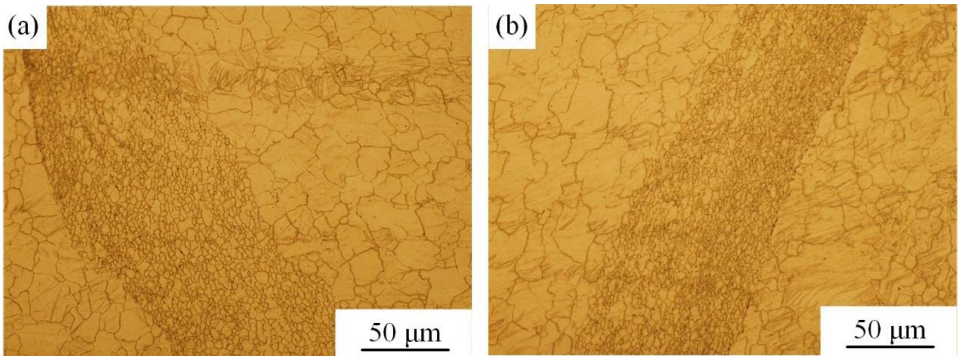

Fig. 7. Typical microstructures of the repaired interfaces by ultrasonic assisted A-PFFSR: (a) A and (b) B in Fig. 5a

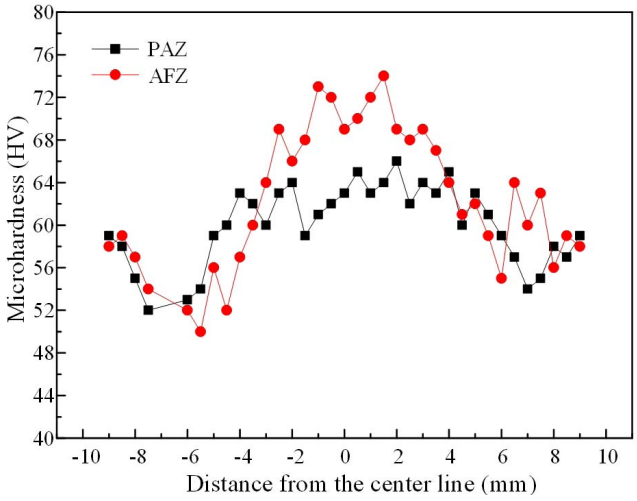

Fig. 8. Microhardness distributions through the thickness direction of the repaired region by ultrasonic assisted A-PFFSR

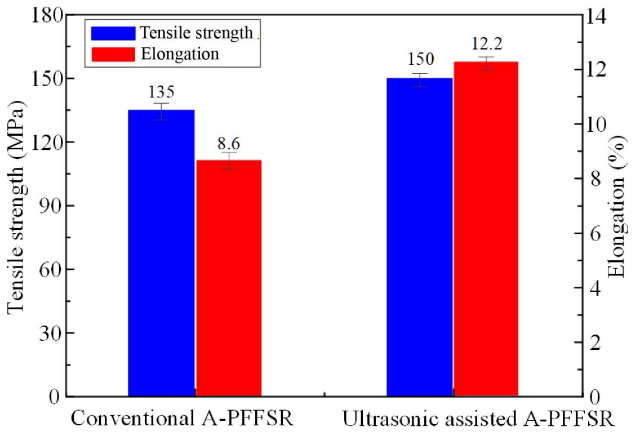

Fig. 9. Tensile properties of the repaired joints using the two repairing processes

atoms, the interfacial defects are eliminated, which can increase the area of load bearing and enhance mechanical properties. Fig. 10 displays the fracture locations and fracture surface morphologies of the repaired joints using the two repairing processes. The fracture locations of the repaired joints all locate at the repairing interfaces between the FZ and the TMAZ. The width of the tensile crack in Fig. 10a is larger than that in Fig. 10b because the interfacial defects between the AFZ and the PFZ are obviously reduced with the ultrasonic. As shown in Fig. 10c, micro fracture surface morphology depicts cleavage-like feature, indicating brittle fracture due to the interfacial defects in the passive filling stage of conventional A-PFFSR. Figs. 10d and e display some dimples and cleavage-like feature, which result from the rapid propagation of the interfacial defects. Compared with the conventional A-PFFSR, these dimples with various sizes and depths appear at the fracture surface morphologies (Figs. 10f-h), which present typical ductile fracture due to good metallurgical bonding at the repairing interfaces induced by the ultrasonic.

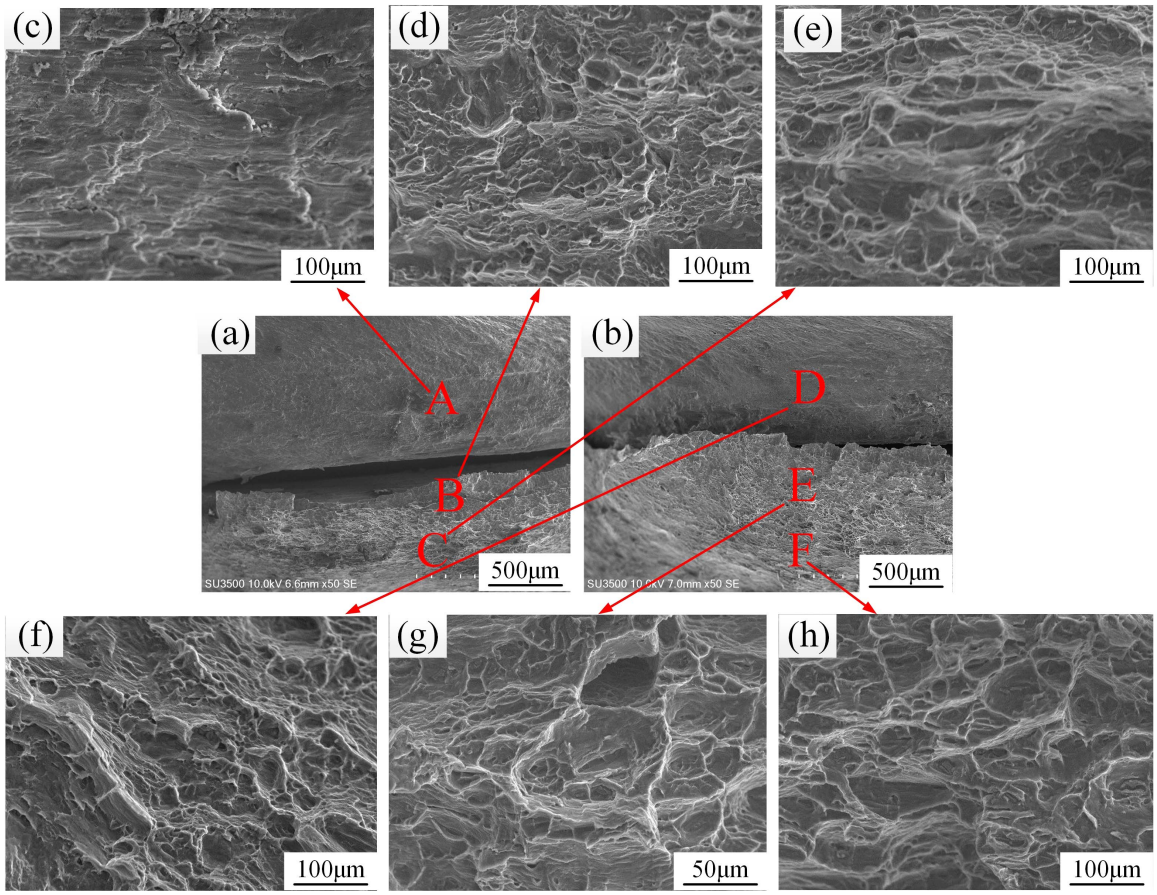

Fig. 10. Fracture surface morphologies of typical repaired joints: macro-morphologies of (a) conventional A-PFFSR and (b) ultrasonic assisted A-PFFSR; micro-morphologies of (c-e) enlarged views marked in Fig. 10a and (f-h) enlarged views marked in Fig. 10b

In summary, the ultrasonic assisted active-passive filling friction stir repairing technique has advantages of good metallurgical bonding, high joint quality and so on, which can be used to the repairing of magnesium and aluminum alloys in aerospace and automotive fields.

4. Summary

Ultrasonic assisted A-PFFSR was proposed to repair the volume defects in the metallic structural parts to achieve the high-quality repairing. The typical keyhole defect in FSWed joint of Mg alloys was successfully repaired without some interfacial defects based on ultrasonic effects. Ultrasonic vibration improved plastic flow of interfacial materials and then eliminated interfacial defects. The equiaxed grains were further refined near the repaired interfaces. Moreover, the improvement of material flow by the ultrasonic could attain the PFZ with a relatively larger thickness, which was beneficial to reducing the repairing passes. The maximum tensile strength of the joint by ultrasonic assisted A-PFFSR were 150 MPa, which was 11% higher than those of conventional A-PFFSR joints, respectively. It can be concluded that ultrasonic assisted A-PFFSR is feasibility and potential in the green remanufacturing fields of metallic structural parts.

Acknowledgements

This work is supported by the National Natural Science Foundation of China (No. 51705339).

REFERENCES

[1] R. Zettler, T. Donath, J.F. Dos Santos, F. Beckman, D. Lohwasser. Adv. Eng. Mater. **8** (6), 487-490 (2006). doi:10.1002/adem.200600062

[2] R. Zettler, A.A.M. Da Silva, S. Rodrigues, A. Blanco, J.F. Dos Santos. Adv. Eng. Mater. **8** (5), 415-421 (2006). doi:10.1002/adem.200600030

[3] B. He, L. Cui, D.P. Wang, H.J. Li, C.X. Liu. Acta Metall. Sin. (English Lett. 2019 (2019). doi:10.1007/s40195-019-00951-x

[4] G. Wang, Y. Zhao, Y. Hao. J. Mater. Sci. Technol. **34** (1), 73-91 (2017). doi:10.1016/j.jmst.2017.11.041

[5] X. Meng, Y. Jin, S. Ji, D. Yan. J. Mater. Sci. Technol. **34** (10) (2018). doi:10.1016/j.jmst.2018.02.022

[6] G.K. Padhy, C.S. Wu, S. Gao. J. Mater. Sci. Technol. **34**, 1-38 (2017). doi:10.1016/j.jmst.2017.11.029

[7] W.F. Xu, Y.X. Luo, M.W. Fu. Mater. Charact. **138**, 48-55 (2018). doi:10.1016/j.matchar.2018.01.051

[8] Z. Liu, S. Ji, X. Meng, Z. Li. Can. Metall. Q. **57** (2), 181-185 (2018). doi:10.1080/00084433.2017.1412555

[9] F. Acerra, G. Buffa, L. Fratini, G. Troiano. Int. J. Adv. Manuf. Technol. **48** (9-12), 1149-1157 (2010). doi:10.1007/s00170-009-2344-9

[10] X. Zhang, Z.P. Cano, B. Wilson, J.R. McDermid, J.R. Kish. Can. Metall. Q. **56** (3), 308-321 (2017). doi:10.1080/00084433.2017.1327500

[11] C. Gunter, M.P. Miles, F.C. Liu, T.W. Nelson. J. Mater. Sci. Technol. **34** (1), 140-147 (2017). doi:10.1016/j.jmst.2017.10.023

[12] S. Ji, X. Meng, L. Ma, H. Lu, S. Gao. Mater. Des. **68** (2015). doi:10.1016/j.matdes.2014.12.009

[13] S. Ji, X. Meng, J. Xing, L. Ma, S. Gao. High Temp. Mater. Process. **35** (8), 843-851 (2016). doi:10.1515/htmp-2015-0063

[14] H. Liu, H. Zhang. Trans. Nonferrous Met. Soc. China. **19** (3), 563-567 (2009). doi:10.1016/S1003-6326(08)60313-1

[15] D.F. Metz, M.E. Barkey. Int. J. Fatigue. **43**, 178-187 (2012). doi:10.1016/j.ijfatigue.2012.04.002

[16] Y.C. Lim, L. Squires, T.Y. Pan, … Z. Feng. Mater. Des. **69**, 37-43 (2015). doi:10.1016/j.matdes.2014.12.043

[17] Y.X. Huang, B. Han, S.X. Lv, … Y. Li. Sci. Technol. Weld. Joi. **17** (3), 225-230 (2012). doi:10.1179/1362171811Y.0000000100

[18] B. Han, Y. Huang, S. Lv, L. Wan, J. Feng, G. Fu. Mater. Des. **51**, 25-33 (2013). doi:10.1016/j.matdes.2013.03.089

[19] Y.X. Huang, B. Han, Y. Tian, … Y. Li. Sci. Technol. Weld. Joi. **16** (6), 497-501 (2011). doi:10.1179/1362171811Y.0000000032

[20] S.D. Ji, X.C. Meng, R.F. Huang, L. Ma, S.S. Gao. Mater. Sci. Eng. A. **664**, 94-102 (2016). doi:10.1016/j.msea.2016.03.131

[21] S. Ji, X. Meng, Y. Zeng, L. Ma, S. Gao. Mater. Des. **97**, 175-182 (2016). doi:10.1016/j.matdes.2016.02.088

[22] R. Huang, S. Ji, X. Meng, Z. Li. J. Mater. Process Technol. **255**, 765-772 (2018). doi:10.1016/j.jmatprotec.2018.01.019

[23] S. Niu, B. Wu, L. Ma, Z. Lv, D. Yan. **d**, 2461-2468 (2018).

[24] Z. Liu, X. Meng, S. Ji, Z. Li, L. Wang. J. Manuf. Process. **31**, 552-559 (2018). doi:10.1016/j.jmapro.2017.12.022

[25] S. Ji, X. Meng, Z. Liu, R. Huang, Z. Li. Mater. Lett. **201**, 173-176 (2017). doi:10.1016/j.matlet.2017.05.011

[26] X.C. Liu, C.S. Wu. Mater. Des. **90**, 350-358 (2016). doi:10.1016/j.matdes.2015.10.131

[27] G.K. Padhy, C.S. Wu, S. Gao. Sci. Technol. Weld. Joi. **20** (8), 631-649 (2015). doi:10.1179/1362171815Y.0000000048

[28] Z. Ma, Y. Jin, S. Ji, X. Meng, L. Ma, Q. Li. J. Mater. Sci. Technol. **35** (1), 94-99 (2019). doi:10.1016/j.jmst.2018.09.022

[29] M. Thomä, G. Wagner, B. Straß, B. Wolter, S. Benfer, W. Fürbeth. J. Mater. Sci. Technol. **34** (1), 163-172 (2017). doi:10.1016/j.jmst.2017.10.022

[30] S. Ji, S. Niu, J. Liu, X. Meng. J. Mater. Process Technol. 2019 (2019). doi:10.1016/j.jmatprotec.2018.12.010

[31] X.C. Liu, C.S. Wu. J. Mater. Process Technol. **225**, 32-44 (2015). doi:10.1016/j.jmatprotec.2015.05.020

[32] W. Li, J. Li, Z. Zhang, D. Gao, W. Wang, C. Dong. Mater. Des. **62**, 247-254 (2014). doi:10.1016/j.matdes.2014.05.028

[33] S.D. Ji, X.C. Meng, L. Ma, S.S. Gao. Int. J. Adv. Manuf. Technol. **87** (9-12), 3051-3058 (2016). doi:10.1007/s00170-016-8734-x

[34] Y. Huang, X. Meng, Y. Xie, J. Li, L. Wan. Compos. Part A, Appl. Sci. Manuf. **112** (April), 328-336 (2018). doi:10.1016/j.compositesa.2018.06.027

[35] M. Guan, Y. Wang, Y. Huang, J. Li. Mater. Lett. **255**, 126506 (2019). doi:10.1016/j.matlet.2019.126506